



# Processing Information from Magnetic Field Sensors in Helmet Mounted Cueing Systems

**A. SZELMANOWSKI, M. WITOŚ, A. PAZUR**

AIR FORCE INSTITUTE OF TECHNOLOGY, Księcia Bolesława 6, Warsaw, Poland

EMAIL: andrzej.szelmanowski@itwl.pl

## ABSTRACT

In the XXI century, magnetic measurements are widely used in many diverse applications. In this paper, we present the practical application of magnetic measurements in the Helmet Mounted Cueing System (HMCS) on board military aircraft. We start with the research problem and proposed solutions (idea). Next, the theoretical basis of the helmet's system operation are described. Herein, we include the characteristics of the Earth's magnetic field and the modeling of this (WMM 2015, IGRF 12, EMM2017), as well as the theory of magnetic field distribution as generated in flat coils, Helmholtz coils and anti-Helmholtz coils. In the later detailed part, we describe the metrological aspects of HMCS applications and the characteristics therein of different magnetometers used in the tests, plus example test results. Finally, we describe ongoing research, while in the summary, we present further research possibilities and potential directions of research in the avionic implementation of magnetic phenomena in HMCS systems.

**KEYWORDS:** magnetic sensors, electromagnetic field, magnetic instruments, magnetic measurements

## 1. Introduction

In the 21st century, the market for magnetometers is the fastest growing among all various sensors. Today, magnetic and electromagnetic measurements are widely used in different applications, e.g. informatics devices (data carriers, smartphones, tablets), processes monitoring systems in cars, metrology (current intensity measurements, encoders), geology, archeology, medicine, aerial and marine reconnaissance and non-destructive testing (Fig. 1).

A wide range of magnetometers are now on the market, their prices are decreasing and metrological parameters are improving. Moreover, new magnetometer applications, designs and developments are coming to light continuously [12,18]

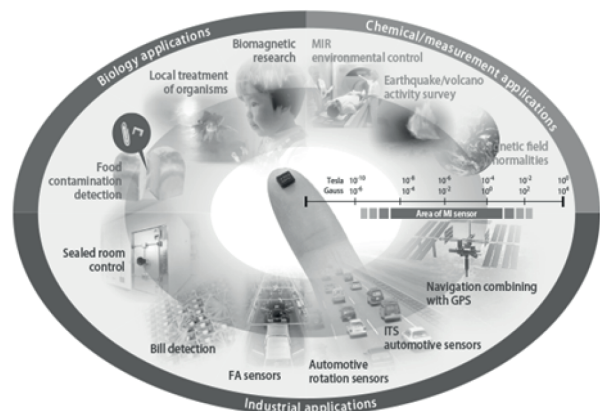


Fig. 1. The varied magnetometer applications [8]

There are many different types of magnetometers designed for different applications. For very small magnetic fields, we can find SQUID sensors; for small magnetic fields - flux-gate sensors; for medium fields - MR sensors; for high magnetic field - Hall sensors (Fig. 2) [18,19].

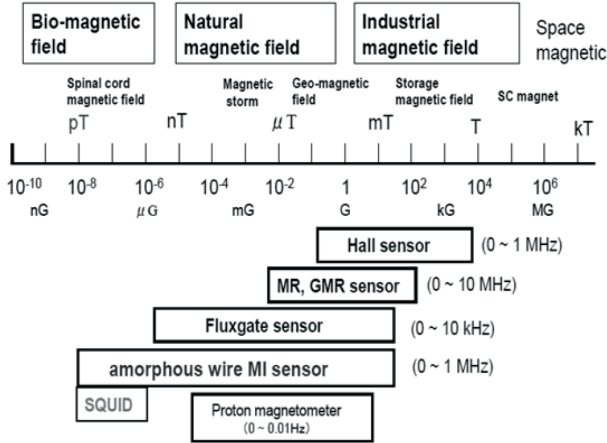


Fig. 2. Typical area of applications for the main magnetic field sensors [own study]

In this article, we present the application of magnetometers in the construction of Helmet Mounted Cueing Systems (HMCS). Several HMCS systems are being currently marketed. These are:

- The JHMCS system, manufactured by Honeywell, found on the F-16 C/D Falcon Fighting (in version Block 52+ PL - in Polish Air Force service). Here, the system of helmet position determination is based on the generation of an artificial reference magnetic field “connected” to the aircraft’s cockpit [15];
- TOPOWL system, used on French and German military helicopters [15];
- NSC-1 ORION system, designed in the Air Force Institute of Technology, as a technology demonstrator dedicated for the W-3PL Głuszec helicopter (Fig. 3) [17].



Fig. 3. W-3PL Głuszec helicopter [own study]

## 2. Research problem

The helmet cueing system is a key element of the weapon control system in modern military aircraft [15]. Its main task is to deliver reliable information about the pilot’s head orientation (within a 6 DOF coordination system). This information is then processed in the mission computer to form a set of control signals for a turret gun (or an optoelectronic surveillance system or line of sight or other guided weapon system). Such signals include azimuth and elevation angles.

A good helmet system ensures achievement of advantage in combat, improves the general performance of the aircraft, increases the chances of completing the mission and ensures the survival of the crew (Fig. 4).

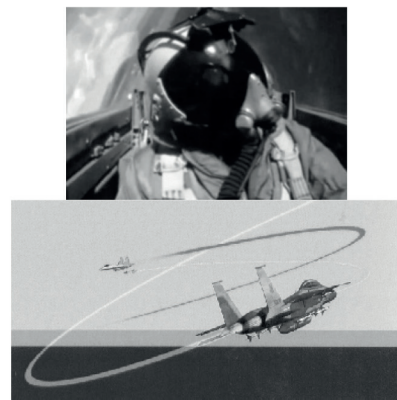


Fig. 4. Advantages of a good helmet system [own study]

The above-mentioned control signals have to be insensitive for the attitude and dynamics of aircraft flight (thus, they have to include corrections). Significant metrological parameters are pilot’s head pitch and yaw angles. Turret gun control disturbance parameters include aircraft roll angle and linear movements of the pilot’s head, in addition to the aircraft’s attitude and variable flight parameters.

The main research problem is how to accurately and quickly measure the spatial position of the helmet in the aircraft’s coordinate system. In other words, the problem involves an interaction between two main coordinate systems (Fig. 5):

- 6 DOF aircraft’s system according to the Earth;
- 6 DOF helmet’s system according to the aircraft.

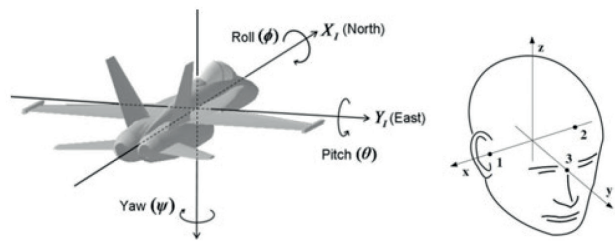


Fig. 5. The two main coordinate systems utilized in current HMCS systems [own study]

This research problem is not trivial as it includes metrological and analytical aspects that arise because the pilot is placed inside an aircraft's cockpit, in a weapon system which performs complex and dynamic motions in space. Example flight parameters of a modern, highly maneuverable aircraft are [15]:

- Speed: up to 2.2 Ma;
- Altitude: up to 12 km above sea level;
- Linear accelerations: up to 8 g (78.5 m/s<sup>2</sup>);
- Angular speeds: up to 1000 degrees/second.

That is why the metrological requirements for a sensor are very demanding. Common demands include:

- Update frequency: min. 240 Hz;
- Latency: max. 3.5 milliseconds (filter off).
- Static accuracy:
  - 0.2 degree RMS for sensor orientation;
  - 0.8 mm RMS for the X, Y, Z position;
- Dynamic accuracy: similar to existing solutions.

Hence, measurement data have to be transferred from a movable head's coordinate system in the form of turret gun control signals - to an immovable turret gun coordinate system afixed within the aircraft. It must be remembered that the turret gun and the pilot's head coordinate systems are not placed in the aircraft's centre of gravity. This last determines the flight trajectory and is central to the aircraft coordinate system.

## 2.1 The idea of the helmet system

For solving the research problem, researchers have proposed the measuring of the slowly changing Earth's geomagnetic field via two vector magnetometers, the first one is placed on the pilot's helmet; the second one is placed inside the aircraft cockpit (and is in use only during the magnetic field distribution mapping process inside the cockpit) (Fig. 6).

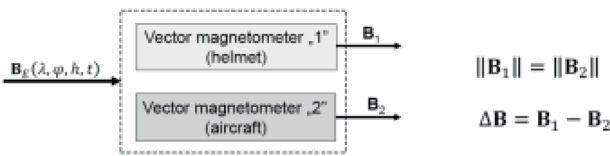


Fig. 6. Idea of magnetic tracking using only the geomagnetic field [own study]

The Earth's magnetic field  $B_E$  is a sum of several contributions (Fig. 7):

- Core field,  $B_{core}$ ;
- Crustal field,  $B_{crust}$ ;
- Combined disturbance field,  $B_{disturbance}$ .

$$B_E(r,t) = B_{core}(r,t) + B_{crust}(r,t) + B_{disturbance}(r,t)$$

$B_{core}$  dominates the field (>95%  $B_E$  at the Earth's surface) with secular variation <100nT/year - this is described by the WMM 2015 and IGRF models [3, 6].  $B_{crust}$  has spatial variations on the order of meters, to thousands kilometers - this is described by the

EMM 2017 model [10].  $B_{disturbance}$  varies both with location and time - this is monitored by SWPC (USA) and INTERMAGNET network stations (around the globe) [9,11].

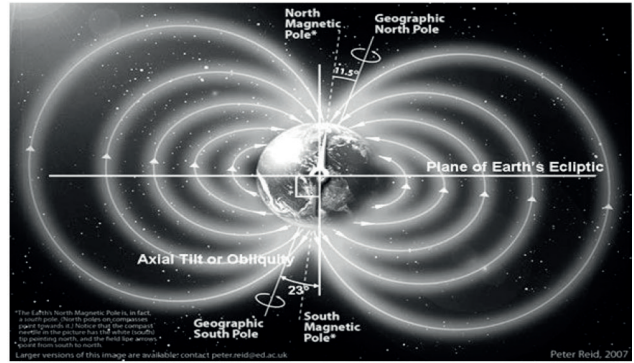


Fig. 7. The Earth's geomagnetic field [own study]

The simple idea of helmet magnetic tracking using only the geomagnetic field was found to be insufficient. In our initial tests, the accuracy of the helmet's position was more than 5 degrees away from true. Hence, such a simple method cannot be applied to the Helmet Mounted Cueing System because of:

- loss of information about small linear movements of the helmet inside the cockpit;
- local homogeneity of the geomagnetic field;
- the negative impact of the "local magnetic field"  $\Delta B_i$ , generated by ferromagnetic components of the aircraft (still and rotating), the on-board electrical networks (DC,AC) and the electrical devices;
- the influence of flight parameters (e.g. linear and angular velocities, acceleration, attitude and spatial position) on  $B_{core}$ ,  $B_{crust}$ ,  $B_{disturbance}$  and measured data  $B_1$  and  $B_2$ .

Therefore, to increase accuracy and make the system doable, a reference signal is needed (Fig. 8). Our researches were realized as two variants:

- with a flat coil supplied by a rectangular electric current signal;
- with a pair of coils in Helmholtz and anti-Helmholtz configuration supplied by a rectangular electric current signal.

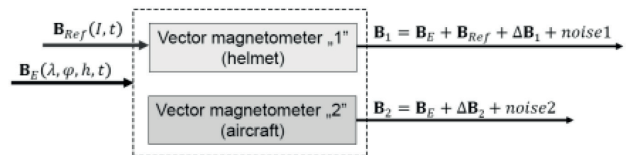


Fig. 8. Concept of magnetic tracking using the geomagnetic field and reference signal [own study]

In the cockpit (test stand), either one flat coil was placed behind the pilot's helmet (NSC-1 ORION system) or a pair of coils (research and development works of the system) were placed on both sides of the helmet, generating a reference magnetic field for the receiver (the helmet's magnetometer).

The flat coil is supplied by rectangular electric current signal (in a current and no-current state). Thus, the pair of coils are successively in the below mentioned states:

- turned off (in no-current state after stabilization of transient states);
- turned on in Helmholtz configuration;
- turned off;
- turned on in anti-Helmholtz configuration.

On the basis of the above mentioned measuring cycle and the applied algorithms of data analysis, the following influences on turret gun control signals are eliminated:

- Earth's geomagnetic field and aircraft's spatial attitude in the geophysical coordinate system;
- dynamics of aircraft flight (linear and angular accelerations);
- magnetic field disturbances generated by aircraft's ferromagnetic elements and DC power supply system.

In the designed prototype of the NSC-1 Orion system, the initial research target was accomplished. The accuracy of helmet control of the turret gun was less than 1 degree.

In order to increase the reliability of helmet's system:

- the technical state of measurement path is monitored on the basis of reference data from the World Magnetic Model WMM 2015 [10]. Input data to WMM2015 model (time, geographical position and altitude of the aircraft) is obtained from the GPS system during the flight or are loaded into the mission computer before the mission;
- periodically (during the maintenance), the magnetic field distribution inside the cockpit is mapped, on this basis, the residual magnetism from aircraft's ferromagnetic elements (the influence of stress magnetism) and changes of coil inductance are evaluated. The magnetic field distribution mapping process and the resulting calibration is done with specific measuring apparatus in an accredited laboratory.

The system, in its developed version, can be supplied by the geomagnetic field parameters and data from on-board systems such as GPS or AHRS.

As an output, we obtain the dynamic correction of the helmet positioning (Fig. 9).

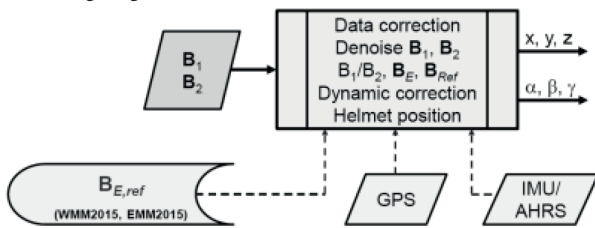


Fig. 9. The concept of helmet dynamic correction measurements [own study]

## 2.2 Theoretical notions

In our first tests, we used a flat coil supplied by a rectangular electric current signal. The field for the circular loop of current  $I$

and radius  $R$  as displaced from the origin by distance  $D$ , as shown in Fig. 10, has magnetic field components given by (1) and (2) [14].

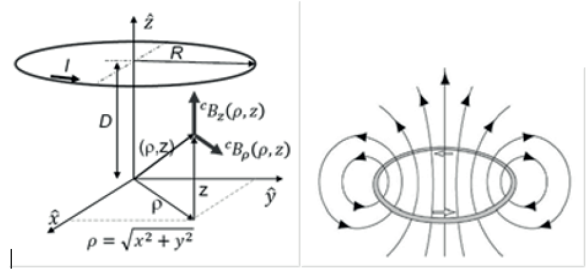


Fig. 10. Cylindrical coordinates for the magnetic field distribution of a single circular current loop of a flat coil [own study]

$${}^c B_r = -\frac{\mu I}{2\pi} \frac{1}{\sqrt{(R+\rho)^2 + (z-D)^2}} \left( \frac{R^2 - \rho^2 - (z-D)^2}{(R-\rho)^2 + (z-D)^2} E(k^2) + K(k^2) \right) \quad (1)$$

$${}^c B_\phi = \frac{\mu I}{2\pi} \frac{z-D}{\sqrt{(R+\rho)^2 + (z-D)^2}} \left( \frac{R^2 + \rho^2 - (z-D)^2}{(R-\rho)^2 + (z-D)^2} E(k^2) + K(k^2) \right) \quad (2)$$

Here,  $\mu$  is a permeability of free space (for air, permeability is approximately equal to that of a vacuum);  $R$  is a radius in the  $xy$  plane,  $k$  is a parameter (3), while  $K$  is the complete elliptic integral of the first kind and  $E$  is the complete elliptic integral of the second kind. The exact values of the complete elliptic integral  $K(k)$  and  $E(k)$  are available in tables.

A Helmholtz coil is a parallel pair of identical circular coils spaced one radius apart and wound so that the current flows through both coils in the same direction. A Helmholtz coil is a device for producing a region of nearly uniform magnetic field with low gradient and low curvature (Fig. 11) [5,13].

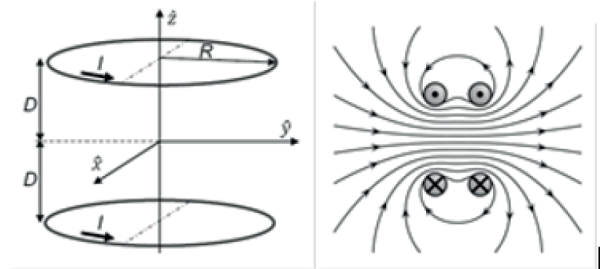


Fig. 11. Magnetic field distribution in Helmholtz coil [own study]

The magnetic field components (4) and (5) of the Helmholtz coil are computed from the sum of the two fields generated by two coils:

$${}^{HC} B_z(\rho, \phi, z) = {}^c B_{z,2}(\rho, \phi, z-D) + {}^c B_{z,1}(\rho, \phi, z+D) \quad (3)$$

$${}^{HC} B_\phi(\rho, \phi, z) = {}^c B_{\phi,2}(\rho, \phi, z-D) + {}^c B_{\phi,1}(\rho, \phi, z+D) \quad (4)$$

Near the origin of the ideal Helmholtz coil (when  $R=2D$ ,  $\rho < 0.2R$ ,  $|z| < 0.2R$ ), components of magnetic field (up to the second order of Taylor series) are described as below:

$${}^{HC}B_{\rho} = 0 + \dots \quad (5)$$

$${}^{HC}B_z = \frac{8}{5\sqrt{5}R} \mu_o I + \dots \quad (6)$$

We can see that the radial component equals to 0 and the longitudinal component depends on the electric current and the coil size (geometry). However, certain conditions must be achieved in order to measure the angular position of the helmet.

An anti-Helmholtz coil is a device for producing a quadruple trap – the field is zero and the gradient is high at the center (Fig. 12). It consists of two identical circular magnetic coils that are placed symmetrically along a common axis, separated by a distance equal to the radius of the coil. Each coil carries an equal electric current in the opposite direction.

The magnetic field components of the anti-Helmholtz coil (8) and (9) are computed from the difference of the fields generated by the two coils [22].

$${}^{aHC}B_{\rho}(\rho, z, \phi) = {}^cB_{\rho,2}(\rho, z - D, \phi) + {}^cB_{\rho,1}(\rho, z + D, \phi) \quad (7)$$

$${}^{aHC}B_z(\rho, z, \phi) = {}^cB_{z,2}(\rho, z - D, \phi) + {}^cB_{z,1}(\rho, z + D, \phi) \quad (8)$$

Near the origin of the ideal anti-Helmholtz coil (when  $R=2D$ ,  $\rho < 0.2R$ ,  $|z| < 0.2R$ ), the situation is as described as below:

$${}^{aHC}B_{\rho} = -2\mu_o I a_1 \rho + \dots \quad (9)$$

$${}^{aHC}B_z = 4\mu_o I a_1 z + \dots \quad (10)$$

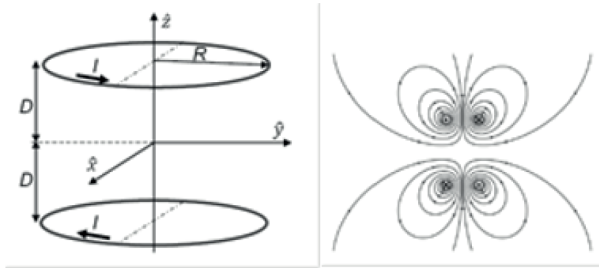


Fig. 12. Magnetic field distribution in Anti-Helmholtz coil [own study]

Certain conditions are necessary for measuring the linear position of the helmet, and in order to obtain the unequivocal representation of the helmet's attitude, as well as reliable data for turret gun control system, the below mentioned assumptions are accepted:

- The pilot's head is placed centrally between the two coils, in a quasi-homogeneous zone of magnetic field for the Helmholtz configuration (non-homogeneity is less than 0,5% and quasi-linear changes of  $B_z$  and  $B_{\rho}$  for the anti-Helmholtz configuration (nonlinearity) is less than 0,5%);
- linear movements of pilot's head are less than 20% of coil's radii;
- angular displacement of pilot's head is in the scope of  $\pm 90^\circ$  yaw,  $\pm 40^\circ$  pitch and  $\pm 10^\circ$  roll angles.

This limitation of pilot's head displacements enables the introduction of the previously presented formulas and components and low-order polynomials (Fig. 13), in the first step of the measurement data analysis. For other sub-ranges, there is a need to add medium and high order polynomials to determine the helmet's true position.

Using the tables of elliptic integrals  $E(k)$  and  $K(k)$  and having the theoretical preparation, conditions are in place to calibrate the measuring path towards mapping the magnetic field distribution

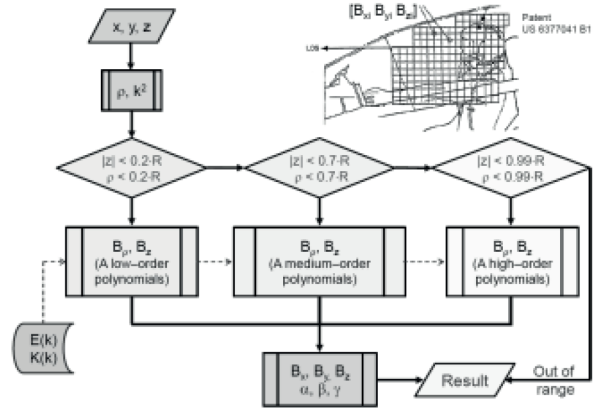


Fig. 13. Measuring path algorithm [own study]

### 2.3 Measurement path

The magnetic field generated by the helmet's system coils is generally assumed to be not higher than 180  $\mu T$ , which is about 300% of Earth's geomagnetic field. Such an assumption enables the use of sensitive magnetometers and the same measurement range to generate useful input data. This:

- ensures the high resolution of measurements;
- eliminates the negative impact from changes of measurement path gain;
- simplifies the measuring data processing in the mission computer.

In the prototype of the Helmet mounted Cueing System, designed and manufactured in the Air Force Institute of Technology in 2010, for the W-3PL Głuszec helicopter, two ADIS 16405 magnetometers (Analog Devices company) were incorporated [1]. The ADIS16405 iSensor device is a complete inertial system that includes a triaxial gyroscope, a triaxial accelerometer and a triaxial magnetometer. Each sensor has its own dynamic compensation formulas that provide accurate sensor measurement.

The signal from the included magnetometers was numerically low-pass filtered so as to reduce measurement path noise and to counter the influence of the electromagnetic field generated by on-board devices supplied by the 400Hz power system.

During the tests, the below-mentioned sensors were used:

- an intelligent electronic compass AMI-305 produced by Aichi [2] that integrates 3MI sensors for obtaining 3-axis magnetic fields;

- a 3-axis inductive magnetometer RM3100 produced by PNI [16], which is characterized by very high temperature and output data rates (ODR) stability;
- a 3-axis TMR magnetometer type FXOS8700 produced by NXP [7] with maximum output data rates of 800Hz;

The Prototype module XEN1210 – a magnetic field sensor based on the Hall effect, equipped with a 24bit digital output and a maximum measurement rate up to 5kHz [21].

In Tab. 1 below, selected parameters of the above-mentioned sensors are presented. Some parameters in the catalogue data are unknown, hence, there is a need for calibration to achieve the required accuracy.

Tab. 1. Selected parameters of the sensors used in tests [own study]

Parameter	Unit	ADIS 16405	AMI 305	RM 3100	FXOS 8700
Type	---	Hall	MI	MI	TMR
Dynamic range	$\mu\text{T}$	$\pm 250$	$\pm 1200$	$\pm 800$	$\pm 1200$
Sensitivity	nT/LSB	50	600	50	100
Axis non-orthogonality	degrees	0.25	0.6	PCB	???
Axis misalignment	degrees	0.5	???	???	???
Sensitivity temperature coefficient ( $1\sigma$ )	ppm/K	600	???	0	0.1%/°C
Bias temperature coefficient	nT/K	50	???	0	800
Nonlinearity	%of FS	0.5	0.5	0.5 ( $\pm 200 \mu\text{T}$ )	1.0
Output noise (no filtering)	nT	125	???	30	<1.5 $\mu\text{T-rms}$
Maximum sample rate for 3-axis mag.	Hz	1200	333	534	800

## 2.4 Laboratory tests

**Variant I:** a flat coil (Fig. 14).



Fig. 14. Test stand with a flat coil [own study]

Referring to the tests conducted, the first variant utilized a flat coil. Herein, the achieved accuracy is less than 2 degrees. Due to the curvilinear character of the magnetic field (Fig. 15), the latency between the measurement and the result is more than 10 ms. The main problem that arose was how to accurately measure linear displacements of the helmet in the non-homogeneous field. We chose to separate the flat coil into two pieces, internal and external, supply electric current to each part and try to determine the linear movements of the helmet in this way. This is an area for further analyzes.

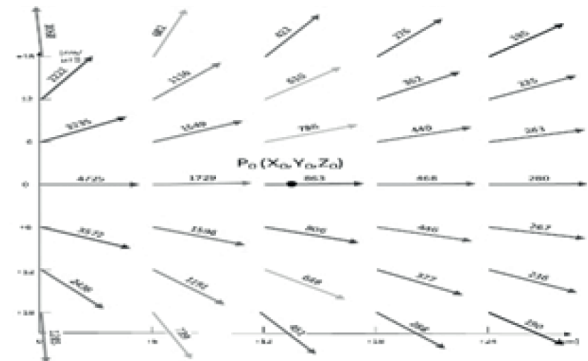


Fig. 15. Magnetic field distribution generated by a flat coil [own study]

**Variant II:** a Helmholtz/anti-Helmholtz coil (Fig. 16).

To achieve better results, we experimented with applying a set of Helmholtz and anti-Helmholtz coils. In the initial tests, the accuracy of the helmet's linear position was less than 1mm, while the helmet's angular position was less than 0,5 degrees and the latency was less than 4 ms.

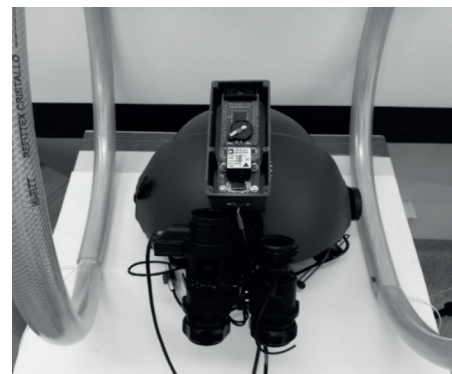


Fig. 16. Test stand with a Helmholtz/anti-Helmholtz coil [own study]

The obtained measurement data were analyzed using the COSMOL MultiPhysics program [4] and the Wolfram Mathematica program [20].

## 3. Conclusion

With the aim of applying magnetic tracking algorithms and verifying the research idea, we utilized the ADIS16405 sensor

(IMU and AHRS system sensors, a3D gyroscope and a 3D accelerometer and 3D magnetometer of the Hall's type) in which the magnetometer has only an auxiliary function – to obtain rough spatial orientation and to compensate for accelerometer and gyroscope error accumulation. The obtained results look promising.

In navigation, most advanced Western aircraft use Fluxgate, AMR and MI type's magnetometers. Their metrological parameters are much better than ADIS16405 or its successor ADIS16480. What is more, 24-bit Q-Hall magnetometers with the sampling frequency  $f_s = 5$  kHz and 15 nT resolution are being marketed, as are very quick 24 and 32-bits ADC converters. The metrological barriers to achieving the research work target, hence, no longer exist.

On the basis of the laboratory tests of the coils that we conducted as well as our prototype Helmet Mounted Cueing System, we see a need for:

- determining unknown magnetometer catalogue data parameters;
- verifying the mechanical vibration influence on real magnetometer metrological parameters.

Further research activities will be orientated to achieving the required functional parameters (update frequency: min. 240 Hz, latency: max. 3.5 milliseconds), and to gaining an understanding of, among others:

- new types of magnetometers and their algorithms verification (differential sets, gradiometers);
- coil power supply signal optimization (sinusoidal signals);
- fast measurement data algorithms optimization.

In the paper, we informed the reader of the prototype Helmet Mounted Cueing System designed in the Air Force Institute of Technology (technology demonstrator). The helmet system is based on magnetic field measurements. Furthermore, in our work, the theoretical basis and metrological aspects of cueing systems were described, as well as were new metrological possibilities resulting from the dynamic development of magnetometers, ADC converters and processors. In pursuing this exploration, our derivations, constructed solutions and gained experiences can be easily transferred to other applications, e.g. control/positioning systems, IPS navigation systems, simulators or virtual reality (VR) systems.

## Bibliography

- [1] ADIS 16405, Analog Devices, Triaxial Inertial Sensor with Magnetometer, datasheet, [www.analog.com](http://www.analog.com) [date of access: 20.01.2020]
- [2] AMI305, Aichi Steel, datasheet, [www.aichi-mi.com](http://www.aichi-mi.com) [date of access: 20.01.2020]
- [3] ARNAUD, C., ET AL.: The US/UK World Magnetic Model for 2015-2020: Technical Report, National Geophysical Data Center, NOAA
- [4] COSMOL Multiphysics® Modeling Software, [www.cosmol.com](http://www.cosmol.com) [date of access: 20.01.2020]
- [5] DE TROYE D.J., CHASE R.J.: The Calculations and Measurements of Helmholtz Coil Fields, Army Research Laboratory, ARL-TN-35, November 1994
- [6] ERWAN T., ET AL.: International Geomagnetic Reference Field: the 12th generation, Earth, Planets and Space 2015, 67, 67-79
- [7] FXSO8700Q, 6-axial sensor with integrated linear accelerometer and magnetometer, technical data, Rev. 8-25 April 2017, [www.nxp.com](http://www.nxp.com) [date of access: 20.01.2020]
- [8] <https://www.aichi-steel.co.jp> [date of access: 20.01.2020]
- [9] <http://www.intermagnet.org> [date of access: 20.01.2020]
- [10] <https://www.ngdc.noaa.gov/geomag/EMM/> [date of access: 20.01.2020]
- [11] <https://www.swpc.noaa.gov/> [date of access: 20.01.2020]
- [12] IEEE SENSORS JOURNAL, Advances in Magnetic Field Sensors, VOL. 10, NO. 6, JUNE 2010
- [13] JAVOR E.R., ANDERSON, T.: Design of Helmholtz Coil for Low Frequency Magnetic Field Susceptibility Testing, Naval Undersea Warfare Center, Division Newport, USA 1998
- [14] KNOEPFEL H.E., Magnetic Fields. A Comprehensive Theoretical Treatise for Practical Use, A Wiley-Interscience Publication, Toronto 2000
- [15] RASH C.: Helmet Displays in Aviation. Helmet Mounted Display. Design Issues for Rotary-Wing Aircraft, USA, Fort Rucker 2009
- [16] RMI3100 Geomagnetic Sensor, datasheet, [www.pnicorp.com](http://www.pnicorp.com) [date of access: 20.01.2020]
- [17] SZELMANOWSKI A.: Helmet Mounted Cueing System NSC-1 ORION for military helicopters with Integrated Avionics System, Air Force Institute of Technology, Warsaw, Poland 2013
- [18] TUMAŃSKI, S.: Modern magnetic field sensors – a review, Electrotechnical Review, R. 89 nr 10.2013
- [19] UCHIYAMA T., ET AL.: Recent Advances of Pico-Tesla Resolution Magneto-Impedance Sensor Based on Amorphous Wire CMOS IC MI Sensor. IEEE Trans. of Magnetics, vol 48(11), 3833-3839, November 2012
- [20] WOLFRAM MATHEMATICA, [www.wolfram.com](http://www.wolfram.com) [date of access: 20.01.2020]
- [21] XEN1210 Magnetic Sensor, datasheet, [www.sensixs.nl](http://www.sensixs.nl) [date of access: 20.01.2020]
- [22] YOUK H.: Numerical study of quadruple magnetic traps for neutral atoms: anti-Helmholtz coils and a U-chip, Department of Physic, University of Toronto 2004